Chapter 4

Dixon Reconstruction and Phase Unwrapping

One of the important applications of phase sensitive reconstruction is Dixon imaging. Multiple images are acquired at different echo times. Linear combinations of these images produce water selective and fat selective images.

This approach is particularly important at lower field strengths, where it is the preferred method of lipid suppression. At 0.5T and below, chemically selective excitation or saturation is impractical since the small fat/water spectral shift would require a very long RF pulse. For example, the minimum time for a spectral-spatial pulse at 0.5T is about 24 ms. Inversion recovery methods become less attractive as the T_1's decrease with decreasing field strength.

4.1 Basic Two Point Dixon Method

The simplest approach uses only two images [1]. The basic assumption is that there are only two components in the image, water and fat. If m_w is the image of the water component, and m_f is the image of the fat component, the combined image at an echo time $T_{E,i}$ is

$$m_i = m_w + e^{-i\omega_f T_{E,i}} m_f \tag{4.1}$$

where we have assumed, for convenience, that we are exactly on the water resonance, so only the lipid component precesses at ω_f. We choose $T_{E,i}$ so that

$$\omega_f T_{E,i} = 0, \pi \bmod 2\pi. \tag{4.2}$$

The two images that result are

$$m_1 = m_w + m_f \tag{4.3}$$
$$m_2 = m_w - m_f. \tag{4.4}$$

We can then combine these to make images that contain only water, or only fat

$$m_w = \frac{1}{2}\left[m_1 + m_2\right] \tag{4.5}$$
$$m_f = \frac{1}{2}\left[m_1 - m_2\right]. \tag{4.6}$$

The problem with this approach is that there are other factors that confound the decomposition. The major factor is the off-resonance frequency shift ω that produces phase errors. Another factor is the T_2 decay of signal at increasing echo times. For spin echoes, the decay may be kept constant by changing the echo time by shifting the refocusing pulse. In gradient-recalled acquisitions, T_2 decay will be a concern. The actual signal for the i^{th} T_E is then

$$\begin{aligned} m_i = {} & m_w e^{-T_{E,i}/T^*_{2,w}} e^{-i\omega T_{E,i}} \\ & + m_f e^{-T_{E,i}/T^*_{2,f}} e^{-i(\omega+\omega_f)T_{E,i}}. \end{aligned}$$

Of these two factors, the problem of the off-resonance frequency ω is by far the most important. The estimation and correction for T_2^* degrades the separation between fat and water slightly, but is of secondary concern. We will ignore this effect here, but see [3] for a detailed analysis of the magnitude of the errors introduced, and the effect on the SNR of the resulting images. Our primary concern here is correcting for the effect of off-resonance frequency.

The two images are then

$$m_1 = (m_w + m_f)e^{i\phi_0} \quad (4.7)$$
$$m_2 = (m_w - m_f)e^{i(\phi_0+\phi)} \quad (4.8)$$

where

$$\phi_0 = -\omega T_{E,1}, \quad (4.9)$$

and the phase due to the precession between two echoes is

$$\phi = -\omega(T_{E,2} - T_{E,1}). \quad (4.10)$$

The initial phase ϕ_0 can be computed from m_1 and eliminated from both terms, so we neglect it. The estimate $\hat{m}_w$ is then

$$\hat{m}_w = \frac{1}{2}(m_1 + m_2) \quad (4.11)$$
$$= \frac{1}{2}(m_w(1 + e^{i\phi}) \quad (4.12)$$
$$+m_f(1 - e^{i\phi})). \quad (4.13)$$

Hence, even for small off-resonance precession angles, the water image is contaminated by a significant component of the fat image. The lipid image is similarly contaminated by the water image. This is illustrated in Fig. 4.1.

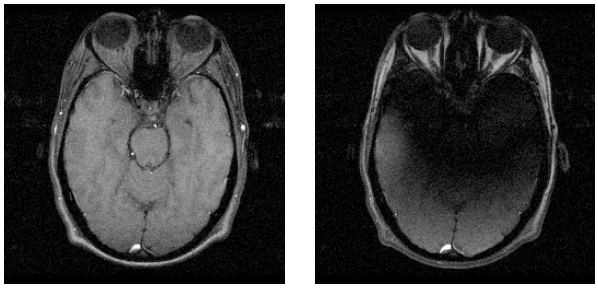

Figure 4.1: A simple two-point Dixon reconstruction of gradient echo data acquired on a 0.5T system. Although the predominant component in the water image is water, and the fat image is fat, there is significant contamination of each by the other. This is due to the off-resonance frequency ω across the head.

4.2 Three Point Dixon Methods

One alternative is to add an additional measurement to allow the off-resonance frequency ω to be estimated. The original proposal [2] was for spin-echo acquisitions, and used measurements at $-\pi$, 0, and π. The echoes were symmetrically distributed about the spin echo.

A better choice that also works for gradient echoes is to pick $T_{E,i}$'s such that

$$\omega_f T_{E,i} = 0, \pi, 2\pi. \quad (4.14)$$

Neglecting ϕ_0 as before, the three images can be written

$$m_1 = (m_w + m_f) \quad (4.15)$$
$$m_2 = (m_w - m_f)e^{i\phi} \quad (4.16)$$
$$m_3 = (m_w + m_f)e^{i2\phi}. \quad (4.17)$$

From images m_1 and m_3 we can estimate

$$2\hat{\phi} = \angle m_1^* m_3. \quad (4.18)$$

We can then phase correct m_2, and combine with m_1 to compute $\hat{m}_w$,

$$\hat{m}_w = \frac{1}{2}(m_1 + m_2 e^{-i\hat{\phi}}) \quad (4.19)$$
$$= \frac{1}{2}((m_w + m_f) \quad (4.20)$$
$$+(m_w - m_f)e^{i\phi}e^{-i\hat{\phi}}) \quad (4.21)$$
$$= \frac{1}{2}((m_w(1 + e^{i(\phi-\hat{\phi})}) \quad (4.22)$$
$$+m_f(1 - e^{i(\phi-\hat{\phi})})). \quad (4.23)$$

A similar expression can be written for $\hat{m}_f$. If $\phi = \hat{\phi}$ the reconstruction is correct. However there is a problem if the phase of ϕ exceeds 2π.

The source of the problem is that the term $2\hat{\phi}$ is itself phase wrapped at 2π. This means that that $\hat{\phi}$ itself wraps at π. After the first wrap of $2\hat{\phi}$

$$\phi - \hat{\phi} = \pi. \tag{4.24}$$

If we substitute this in to Eq. 4.23 we get

$$\begin{aligned} \hat{m}_w &= \frac{1}{2}(m_w(1 + e^{i\pi}) && (4.25)\\ &\quad + m_f(1 - e^{i\pi})) && (4.26)\\ &= \frac{1}{2}(m_w(1 + (-1)) && (4.27)\\ &\quad + m_f(1 - (-1))) && (4.28)\\ &= m_f! && (4.29) \end{aligned}$$

This means that each time $2\hat{\phi}$ wraps by another 2π, water and fat swap. This is an objectionable artifact. Another consequence is that, even if the two do separate properly, you can't tell which will be the water image. This is easily detectable, but unfortunate, since water is usually the image of interest. Figure 4.2 demonstrates the water/fat switching due to a 2π phase wrap in $2\hat{\phi}$.

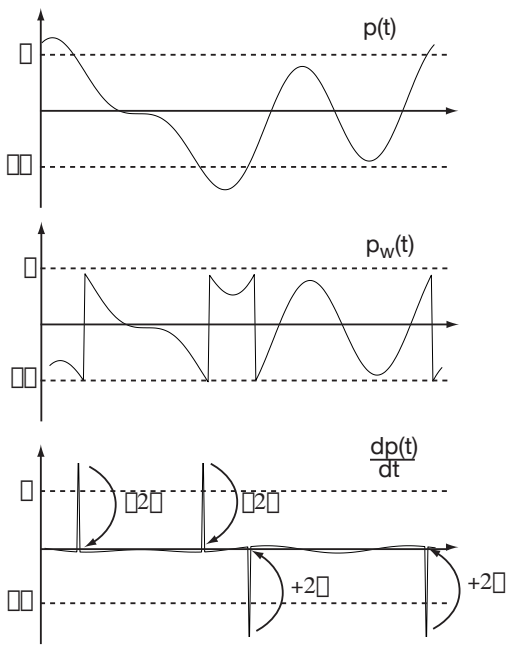

Figure 4.3: A 1D phase unwrapping example. The initial phase waveform has values outside of $\pm\pi$ (top). The wrapped phase $\angle e^{ip(t)}$ then has 2π phase jumps where the $p(t)$ crosses the $\pm\pi$ boundaries (center). If we differentiate $p(t)$ these jumps become impulses of amplitude $\pm 2\pi$. If we subtract or add 2π to bring these points into the $\pm\pi$ range, and then integrate the result, we recover $p(t)$, but with a 2π shift of the entire waveform.

4.3 2D Phase Unwrapping

Two-dimensional phase unwrapping is in general a hard problem. Much of the work in phase unwrapping has been done in Synthetic Aperture Radar (SAR) imaging, where the phase information is used to improve range resolution. SAR data sets typically have hundreds to thousands of phase wraps. The phase unwrapping problem in MRI is relatively easy by comparison, with tens of phase wraps in extreme cases, and typically less than ten. In spite of this, phase unwrapping still fails occasionally, so this is an area that could still use improvement. The algorithms tend to rely on heuristics to decide how to proceed with the unwrapping. As such, the algorithms can be fairly intricate. A description of a large number of different algorithms is presented in [5], and "C" code implementations are available on the Wiley ftp server.

The basic idea of phase unwrapping in 2D is very similar to phase unwrapping in one dimension. Fig. 4.3 illustrates the basic idea in one dimension. The points at which the signal wraps are identified by differentiating the phase function, and looking for samples with values close to $\pm 2\pi$. The samples are wrapped back into the $\pm\pi$ range. Then, integrating restores the original waveform, with a possible offset of a multiple of 2π.

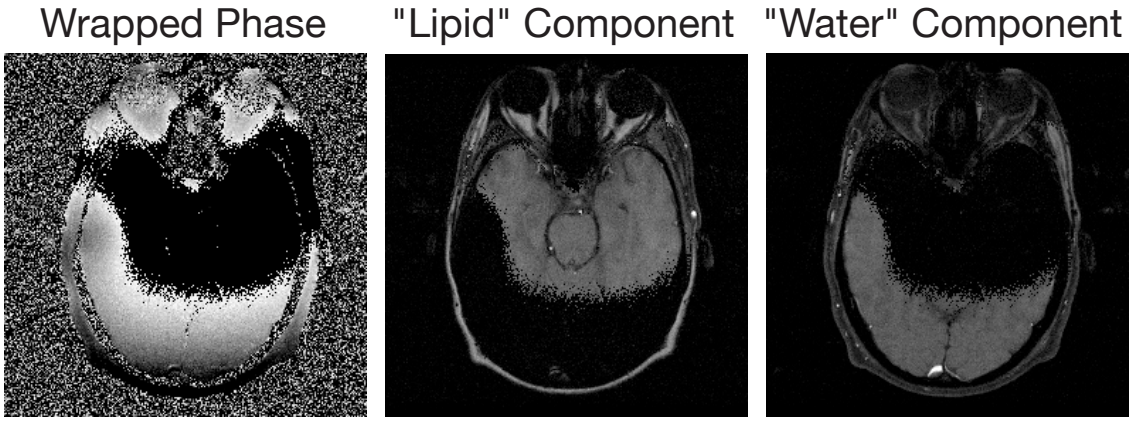

Figure 4.2: A 3-point reconstruction of the data shown in Fig. 4.1. The phase $\hat{\phi}$ wraps, which causes the water and fat components of the images to switch.

The same idea applies in 2D. The phase difference is integrated along a path, and the 2π phase jumps are taken out. The major issue is how to define the path. There are two basic principles. First, the unwrapping should be path independent. This is illustrated in Fig. 4.4. Integrating the phase differences from point A to point B should be the same for any path we take. In addition, integrating around a closed path should be zero.

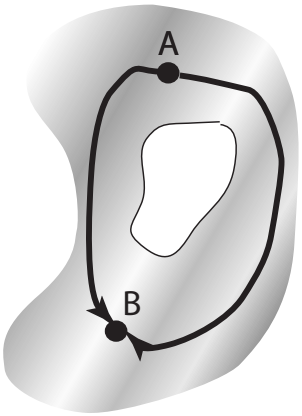

Figure 4.4: In 2D phase unwrapping, the result integrating the phase differences from point A to point B should be independent of the path. In addition, integration around a closed path should be zero.

There are a several areas that cause problems, where these conditions don't hold, and the phase unwrapping fails. One is low signal areas where the phase data is random. Another is areas where the spatial frequencies of the phase map are higher than the resolution of the image. A third problem is unconnected regions.

There are many different algorithms that address these problems. Here we will briefly describe two. The first is based on a quality map of the phase data. The algorithm tries to unwrap using the best data it can find, first. Many different functions have been proposed for quality maps. One is the minimum gradient. Another is the minimum variance of the gradient. The idea is to pick a pixel to start unwrapping, and then region grow by including the border pixel with the best quality value. This is a simple approach that works remarkably well.

Another important class of unwrapping algorithms

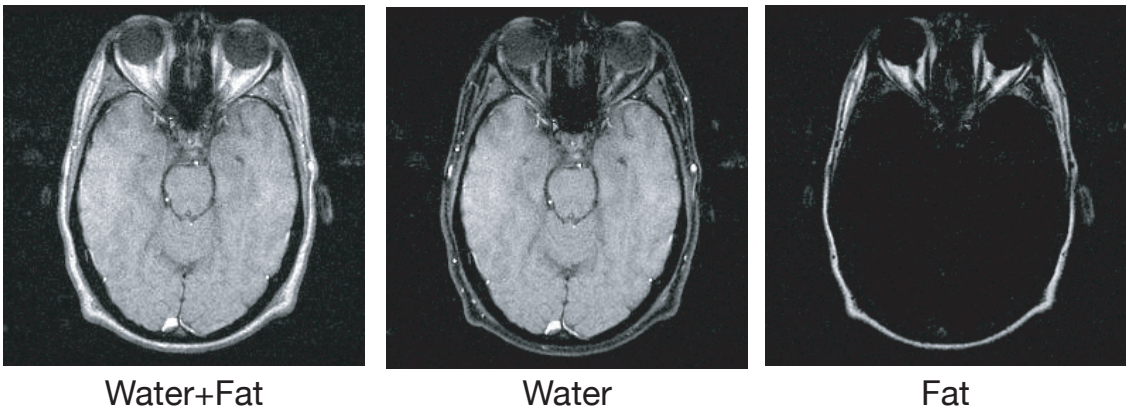

Figure 4.5: A 3-point reconstruction of the data shown in Fig. 4.1 after the phase has been successfully unwrapped.

is based on branch cuts. The idea here is to first identify the points in the phase map that violate the requirement that the integrated phase difference around a closed path is zero. These points are called *residues*. Since we are working on a discrete grid, these residues are discrete, and are conceptually located at the intersection of four image pixels. They can be found by integrating around each 2×2 element of the phase data. Once the residues are found, they are grouped into pairs or sets by *branch cuts*. If a positive residue and a negative residue are connected, and we integrate around the pair, the result is zero. Thus, as long as we don't integrate across a branch cut, we have path independence. Once all the residues have been paired up, and the unpaired residues connected to the image edge, we can unwrap with any path that doesn't cross a branch cut.

Once the phase $2\hat{\phi}$ has been successfully unwrapped, $\hat{\phi}$ has also been unwrapped, and the phase compensated estimates of $\hat{m}_w$ and $\hat{m}_f$ can be unambiguously computed. The result for the data set that was unsuccessfully decomposed into fat and water in Fig. 4.2 is shown properly separated in Fig. 4.5 after unwrapping $2\hat{\phi}$ using a branch cut algorithm. A more challenging problem is shown in Fig. 4.6. The rapid phase changes

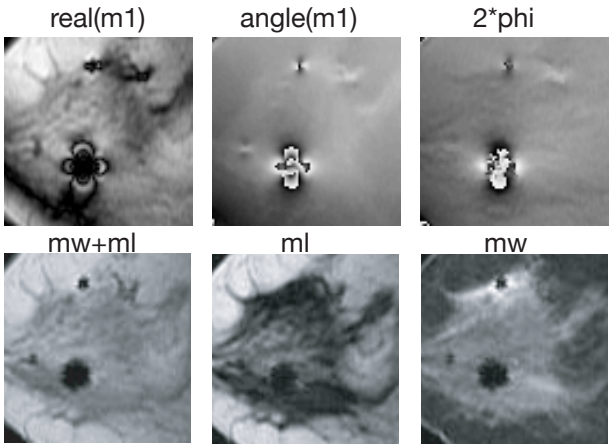

Figure 4.6: Phase artifacts produced by a needle. These are successfully unwrapped, and a properly separated water and fat images produced.

would cause water/fat switching. However, after phase unwrapping with a quality map algorithm, water and fat are properly separated.

4.4 Two Point Dixon, Revisited

Once we understand the idea of three-point Dixon we look back at the two-point approach and effec-

tively accomplish the same thing with only two measurements [6,7]. The main function of the third measurement m_3 in Eq. 4.17 is to allow the estimation of $2\hat{\phi}$ by computing

$$2\hat{\phi} = \angle m_1^* m_3. \tag{4.30}$$

We can also do this with

$$2\hat{\phi} = \angle (m_1^* m_2)^2. \tag{4.31}$$

This effectively synthesizes the third three-point Dixon measurement from the two-point data set. The reason we need to do this using $m_1^* m_2$ is that water and fat have opposite polarities, and that would appear in the phase estimate. By squaring the phase difference, water and fat are again in phase, and we can extract the off-resonance component of the phase. While this is a great idea, in practice its use is limited due to the performance at pixels that have a contribution from both water and fat. Since fat shifts in the readout direction in a 2DFT acquisition, this includes pixels on the fat/water boundary. At these points fat and water interfere, resulting in phase anomalies, and separation failures.

4.5 Conclusion

Three-point Dixon methods provide an effective means of fat/water imaging. Since the fat/water difference frequency is in the order of susceptibility shifts, the off-resonance phase estimate $2\hat{\phi}$ must be unwrapped to avoid water and fat switching. A number of different phase unwrapping routines may be used, and work well. However, there still are occasional failures.

4.6 References

1. W.T. Dixon, Simple Proton Spectroscopic Imaging, *Radiology*, **153**:189-194, 1984.

2. G.H. Glover and E.Schneider, Three-Point Dixon Technique for True Water/Fat Decomposition with B_0 Inhomogeneity Correction,*Magn. Reson. Med*, **18**(2):371–383, 1991.

3. G.H. Glover, Multipoint Dixon Technique for Water and Fat Proton and Susceptibility Imaging, *J. Magn. Reson. Imag.* **1**(5):512–530, 1991.

4. Y. Wang, D. Li, E.M. Haacke, and J.J. Brown, A Three Point Dixon Methods for Water and Fat Separation Using 2D and 3D Gradient Echo Techniques, *J. Magn. Reson. Imag*, **8**(3):703–710, 1997.

5. D.C. Ghiglia and M.D. Pritt, Two-Dimensional Phase Unwrapping: Theory, Algorithms, and Software, Wiley, 1998.

6. T.E. Skinner and G.H. Glover, An Extended Two-Point Dixon Algorithm for Calculating Separate Water, Fat, and B_0 Images, *Magn. Reson. Med*, **37**(4):628-630.

7. B.D. Coombs, J. Szumowski, and W. Coshow, Two Point Dixon Technique for Water-Fat Signal Decomposition with B_0 Inhomogeneity Correction,*Magn. Reson. Med*,**38**(6):884-889.